

A molecular information ratchet

Viviana Serreli¹, Chin-Fa Lee¹, Euan R. Kay¹ & David A. Leigh¹

Motor proteins and other biological machines are highly efficient at converting energy into directed motion and driving chemical systems away from thermodynamic equilibrium¹. But even though these biological structures have inspired the design of many molecules that mimic aspects of their behaviour^{2–15}, artificial nanomachine systems operate almost exclusively by moving towards thermodynamic equilibrium, not away from it. Here we show that information about the location of a macrocycle in a rotaxane—a molecular ring threaded onto a molecular axle—can be used, on the input of light energy, to alter the kinetics of the shuttling of the macrocycle between two compartments on the axle. For an ensemble of such molecular machines, the macrocycle distribution is directionally driven away from its equilibrium value without ever changing the relative binding affinities of the ring for the different parts of the axle. The selective transport of particles between two compartments by brownian motion in this way bears similarities to the hypothetical task performed without an energy input by a ‘demon’ in Maxwell’s famous thought experiment^{16–19}. Our observations demonstrate that synthetic molecular machines can operate by an information ratchet mechanism^{20–22}, in which knowledge of a particle’s position is used to control its transport away from equilibrium.

Maxwell originally conceived his thought experiment, which leads to a non-equilibrium distribution of thermal energy^{16,17} (temperature demon¹⁹) or brownian particles¹⁸ (pressure demon¹⁹), to illustrate the statistical nature of the second law of thermodynamics. But modern synthetic chemistry allows us to consider his idea from a very different perspective: rather than test the second law by attempting to reduce entropy in an isolated system, how can information transfer between a particle and a ‘gatekeeper’ be accomplished non-adiabatically to form a mechanism for a working brownian motion nanomachine?

This question inspired the design of rotaxane **1** (Fig. 1), which consists of a dibenzo-24-crown-8-based macrocycle mechanically locked onto a linear thread by bulky 3,5-di-*t*-butylphenyl groups situated at either end. (For an outline of the synthesis, with 25 steps in the longest linear sequence, see Supplementary Information.) An α -methyl stilbene unit divides the molecule into two ‘compartments’. When this unit adopts the *E*-stilbene isomeric form, the macrocycle can move randomly along the full length of the thread by brownian motion; in contrast, the *Z*-isomer provides a non-traversable steric barrier²³ that traps the macrocycle in one or other of the two compartments. The α -methyl stilbene ‘gate’ is asymmetrically positioned on the thread between two ammonium groups (monobenzyl ammonium, mba; dibenzyl ammonium, dba) that each bind the crown ether macrocycle non-covalently with rather similar affinities^{24,25} but are distinguishable for the purposes of monitoring the system. Photoinduced switching between the open (*E*-) and closed (*Z*-) forms of the gate can occur either through direct photon absorption by the α -methyl stilbene chromophore, or indirectly via energy transfer from the excited state of a triplet photosensitizer. The former is a minor pathway under our experimental conditions (irradiation at

350 nm wavelength) because the triplet sensitizers employed absorb far more strongly at this wavelength than α -methyl stilbene.

For a change in the distribution of the ring between the two compartments of **1** to be established, the stilbene gate needs to be closed for much of the time. This is accomplished by operating the machine in the presence of benzil (PhCOCOPh); the benzil-sensitized photo-stationary state (PSS) of α -methyl stilbene is typically 82:18 *Z:E* (ref. 26; model compounds used to design **1** all exhibited similar PSS ratios at 350 nm in various solvents, see Supplementary Information). To open the gate preferentially when the macrocycle is in the left-hand (dba) compartment a different photosensitizer, which produces a lower *Z:E* ratio for α -methyl stilbene than benzil, must be associated with the macrocycle to ‘signal’ its position and open the gate. We chose benzophenone (PhCOPh) for this purpose, as it gives a 55:45 *Z:E* PSS ratio²⁶ for α -methyl stilbene and as a substructure it could readily be incorporated into a dibenzo-crown ether (see **1**, Fig. 1). As energy transfer is distance dependent, the rates and efficiencies of the intramolecular photosensitized reaction of dba-*Z*-**1** to *E*-**1** should be very different to that of mba-*Z*-**1** to *E*-**1**, whereas the intermolecular photosensitized isomerization with benzil should be relatively independent of the position of the macrocycle. It may seem counter-intuitive that one can drive the macrocycle distribution away from its equilibrium value without ever changing the binding properties of the ring or either of the two ammonium groups that serve as binding sites. But if conditions are chosen so that the benzil-sensitized reaction dominates (gate closed) when the ring is in the mba compartment (that is, held far from the gate), whereas the benzophenone-sensitized isomerization dominates (gate open) when the ring is in the dba compartment (that is, held near to the gate), then this is precisely what should happen.

The system’s operation is shown in Fig. 1, with the results obtained reported in Fig. 2 and Fig. 3 (see Supplementary Information for additional data). The macrocycle shuttles between the ammonium binding sites of the two co-conformers of *E*-**1** shown in Fig. 1 slowly on the proton nuclear magnetic resonance (¹H NMR) timescale, and so two sets of signals, one for each translational form, are observed in the ¹H NMR spectrum of *E*-**1** (Fig. 2b). The relative integration of these peaks gives the distribution of the macrocycle between the compartments at equilibrium (gate open). The ratio is 65:35 dba:mba in CD₃OD at 298 K, as illustrated by the H_s proton signal (corresponding to the dba binding site occupied) and the H_{s'} proton signal (corresponding to the mba binding site occupied) in the partial spectrum shown in Fig. 3c. Irradiation (350 nm, CD₃OD, 298 K) of the rotaxane isomerizes the α -methyl stilbene unit, giving various amounts of the three diastereomers, dba-*Z*-**1**, mba-*Z*-**1** and *E*-**1**. As with the dba:mba distribution, the *Z:E* ratio can be readily established by the relative integration of various signals (for example, H_{k+k'} and H_{k+l'} or H_{l+l'} and H_{l+l'} shown in Fig. 2b and c, or H_{s+s'} and H_{s+s'} shown at points I–IV in Fig. 3c).

Starting from pristine *E*-**1** and with no benzil present (point I, Fig. 3a), irradiation at 350 nm (CD₃OD, 298 K) interconverts the three diastereomers of **1**, ultimately leading to a 38:21:41

¹School of Chemistry, University of Edinburgh, The King’s Buildings, West Mains Road, Edinburgh EH9 3JJ, UK.

dba-*Z*-1:mba-*Z*-1:*E*-1 photostationary state (that is, point II, Fig. 3a). While the *Z*:*E* ratio of **1** changes from 0:100 to 59:41 during this part of the experiment, the dba:mba ratio remains almost invariant at 65:35 (see below for an explanation of the transient small increase in the population of the dba compartment during the first 5 min of irradiation, Fig. 3b).

After 25 min irradiation of **1** (point II, Fig. 3a), one equivalent of benzil was added and irradiation resumed. The 1:1 combination of the benzil and benzophenone-crown ether photosensitizers produces a higher *Z*:*E* α -methyl stilbene PSS ratio (66:34, point III, Fig. 3a) than the benzophenone-crown ether alone. This modest change is accompanied for the first time, however, by a decrease in the population of the dba-compartment (dba:mba, 58:42). The amount of external sensitizer required for **1** to operate at greatest efficiency is determined by several factors, which include the relative absorptions of the different chromophores, the relative efficiencies of energy transfer from the chromophores to the α -methyl stilbene and between the triplet sensitizers themselves, and the concentration of the external sensitizer. Five equivalents of benzil proved sufficient to increase the *Z*:*E* ratio of **1** at the PSS to 80:20, essentially the same as if no benzophenone was present. Addition of more benzil did not further increase the *Z*:*E* ratio (point IV, Fig. 3a). At this maximum value the dba:mba ratio is 45:55 (dba-*Z*-1:mba-*Z*-1:*E*-1, 32:48:20); nearly one-third of the macrocycles which occupied the more energetically favourable dba compartment at equilibrium (or the PSS

obtained in the absence of benzil) have been pumped into the compartment with the less favourable mba binding site.

To confirm the mechanism by which the macrocycle distribution in **1** is driven away from its equilibrium value, the same photochemical experiment was performed on a rotaxane with a crown ether lacking a photosensitizer unit (Fig. 4). Rotaxane **2** was irradiated (350 nm, CD₃OD, 298 K) in the presence of the unthreaded benzophenone-derivatized crown ether, **3**, both with and without benzil so that isomerization by each photosensitizer could only occur intermolecularly. The results are shown graphically in Fig. 4. Although, like **1**, the *Z*:*E* ratio of **2** changes from 0:100 to 80:20 during the photochemical experiment, the distribution of the macrocycle between the two compartments in rotaxane **2** remains virtually unchanged from its equilibrium value of 52:48 dba:mba. (We note that the underderivatized dibenzocrown ether in **2** is slightly less discriminatory for the different ammonium binding sites than the benzophenone-macrocycle in **1**, hence the different dba:mba ratio.)

A small and short-lived increase in the population of macrocycles present in the dba-compartment is observed during the initial irradiation of *E*-1 in the absence of benzil (Fig. 3b). This occurs because the photosensitized isomerization reaction is a much more frequent occurrence when the photon is absorbed by the macrocycle on the dba binding site of *E*-1, which results in dba-*Z*-1 forming more rapidly from *E*-1 than mba-*Z*-1. Equally, however, dba-*Z*-1, in which the photosensitizer is trapped close to the gate, is converted back to

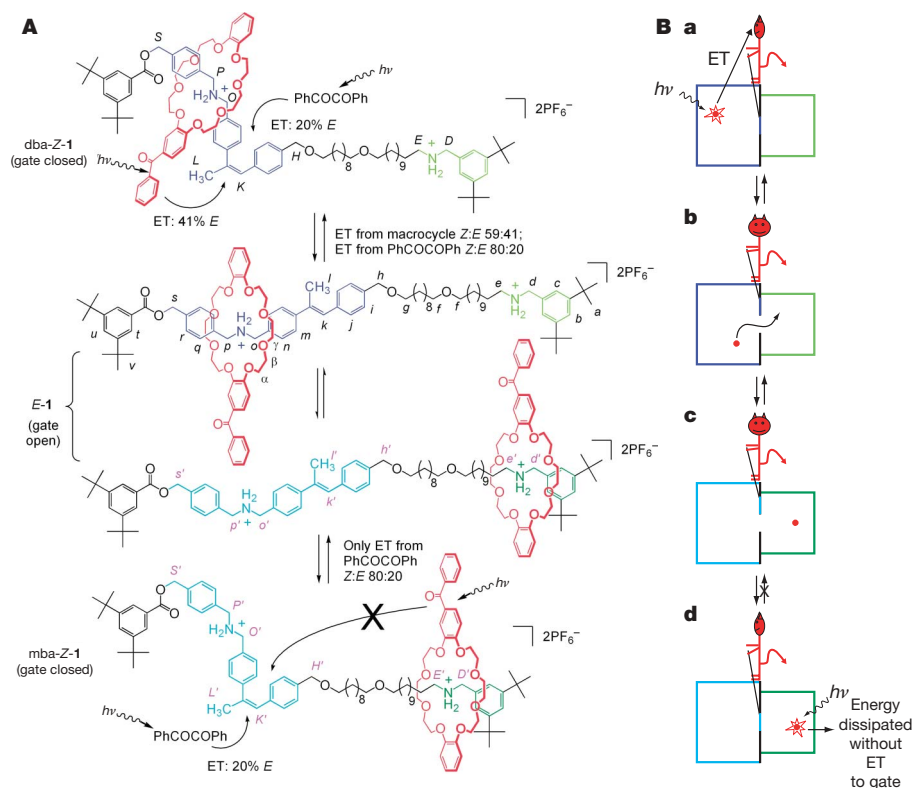


Figure 1 | A photo-operated molecular information ratchet. A, Irradiation of rotaxane **1** (1 mM) at 350 nm in CD₃OD at 298 K interconverts the three diastereomers of **1** and, in the presence of benzil (PhCOCOPh), drives the ring distribution away from the thermodynamic minimum, increasing the free energy of the molecular system without ever changing the binding strengths of the macrocycle or ammonium binding sites. For clarity, the photoinduced energy transfer (ET) pathways are only illustrated for the *Z*- (gate closed) forms of **1** although the same processes occur for the equivalent *E*- (gate open) translational isomers. When the macrocycle is on the mba binding site (green), intramolecular ET from the macrocycle is inefficient and intermolecular ET from benzil dominates (the cross on the intramolecular ET arrow is used to indicate that it is a rare event compared to

other relaxation pathways). When the macrocycle is on the dba binding site (blue), both ET mechanisms can operate efficiently. The amount of benzil present determines the relative contributions of the two ET pathways and thus the nanomachine's effectiveness in pumping the macrocycle distribution away from equilibrium (see Fig. 3). The mechanism requires the shuttling of the ring between the two ammonium groups in *E*-1 to be slow with respect to the lifetime of the macrocycle-sensitizer triplet excited state. The Greek and italicized lettering are the proton assignments for the ¹H NMR spectra shown in Figs 2 and 3. **B**, Cartoon illustration of the operation of **1** in terms of a non-adiabatic Maxwellian pressure demon^{18,19}. See text for details.

E-1 much faster than is *mba-Z-1*, and thus the statistical balance of macrocycles present in the *dba-* and *mba-* compartments is quickly restored as the reaction proceeds. This phenomenon illustrates the fascinating interplay between the statistical balance of the position of the particle (*dba/mba* compartment) and the ‘statistical balance’ of the position of the gate (open *E*-stilbene/closed *Z*-stilbene) in the operation of **1**. Moving either one of these normally orthogonal chemical features away from its ‘equilibrium’ value moves the other one away too.

By relating the net change of position of the macrocycle between the two compartments in an ensemble of **1** to the sorting of ideal gas particles between two boxes of different volume, it can be shown (see Supplementary Information) that the free-energy change on driving the distribution away from equilibrium is given by equation (1), where N is the total number of particles, x_1 is the final mole fraction of particles in the *dba* compartment and y_1 is the equilibrium mole fraction of particles in *dba*.

$$\Delta G = Nk_B T \left[x_1 \ln \frac{x_1}{y_1} + (1 - x_1) \ln \frac{(1 - x_1)}{(1 - y_1)} \right] \quad (1)$$

Using the experimental values obtained for **1** (Fig. 3a), namely $x_1 = 0.45$ and $y_1 = 0.65$, this gives a free-energy change of $\Delta G = 0.083 RT \text{ J mol}^{-1}$.

Note that during the operation of **1** the photons are not raising the energy of a transported component as typically happens in other artificial nanomachines. Instead, the light energy is used to power an information transfer process. As in Maxwell’s thought experiment, information about the location of the particle is used to selectively and transiently lower a kinetic barrier and thereby perturb the particle distribution without energetically favouring one compartment over the other at any stage. The effectiveness of the mechanism in **1** depends directly upon the efficiency of the energy transfer to the closed gate from the excited state of a benzophenone-macrocycle that

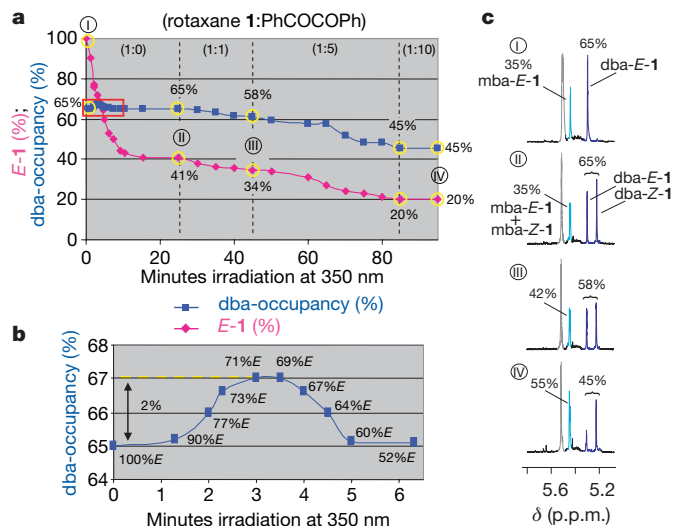


Figure 3 | Operation of a molecular information ratchet. **a**, Change in the *E:Z* ratio (*E-1* (%)), the amount of the ‘open gate’ form of the sample, shown by purple diamonds) and the *dba:mba* ratio (*dba-occupancy* (%)), shown by dark blue squares) that occurs during irradiation of **1** at 350 nm in CD_3OD , 298 K: I, pristine *E-1*; II, after 25 min (PSS), no added benzil; III, after a further 20 min (PSS) with 1 equiv. benzil; IV, after a further 40 min with 5 equiv. benzil plus a further 15 min (PSS) with 10 equiv. benzil. A small amount of photodegradation (<2%) occurs over the course of the experiment, and the error in the final *E:Z* and *dba:mba* ratios is $\pm 2\%$. **b**, Expansion showing the small increase (2–5%, see Supplementary Information) in *dba* compartment occupancy that occurs during the first five minutes of irradiation in the absence of benzil. **c**, ^1H NMR spectral window ($H_{s'+s}$, H_s and $H_{s'}$, 600 MHz, CD_3OD , 298 K) in which the changes in both the *E:Z* and *dba:mba* ratios can be seen during the photochemistry experiment.

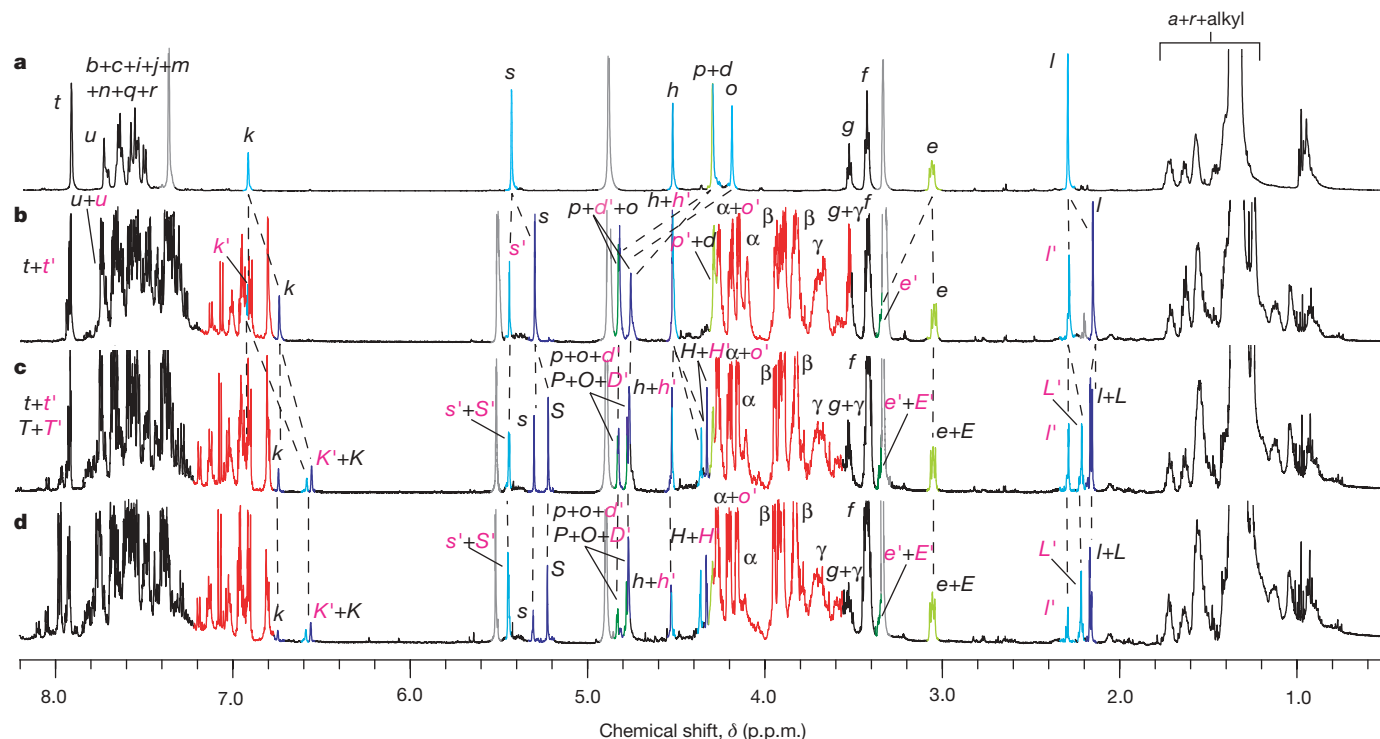


Figure 2 | ^1H NMR spectra (600 MHz, CD_3OD , 298 K) of a working nanomachine. **a**, Thread (*E*-diastereomer); **b**, *E-1*; **c**, **1** at the 350 nm photostationary state (*dba-Z-1:mba-Z-1:E-1*, 38:21:41); **d**, **1**+benzil (10 equiv.) at the 350 nm photostationary state (*dba-Z-1:mba-Z-1:E-1*, 32:48:20). Resonances are coloured and the lettering assigned according to Fig. 1: macrocycle, red; occupied *dba* binding site, dark blue;

unoccupied *dba* binding site, light blue; occupied *mba* binding site, dark green; unoccupied *mba* binding site, light green. The overlapping aromatic ring signals above 7.2 p.p.m. are not distinguished in this way. Residual non-deuterated solvents are shown in light grey (the signal at 5.5 p.p.m. is CH_2Cl_2).

is located in the left-hand compartment (dba-Z-1; Fig. 1B, a), compared to that from one in the right-hand compartment (mba-Z-1; Fig. 1B, d).

The second law of thermodynamics demands that an energetic cost be paid for moving a particle distribution away from equilibrium. In both Maxwell's thought experiment and our molecular system, it is the subtle requirement for energy dissipation during the transfer of information that meets this requirement. In practice, the conversion of photonic energy to heat occurs in several places during the photochemical excitation, energy transfer and thermal relaxation processes in the operation of **1**, meaning that the second law is easily satisfied. However, the heat loss in most of these instances could theoretically be eliminated by changing details of the experimental design (for instance, benzil would be unnecessary if **1** could be modified so that the open form of the gate was able to exergonically relax to the closed form). The one part of the mechanism where loss of heat to the environment appears unavoidable is during the isomerization of the gate by the sensitizer attached to the macrocycle. Photochemical excitation is an extremely rapid process and occurs without changes in molecular geometry (the Franck-Condon principle). For olefin photoisomerization to occur, the initial 'vertically' excited state must relax to its preferred geometry (known as the 'perpendicular' state), which is somewhere intermediate between the *Z* and *E* forms. A further rearrangement of this nuclear configuration to the final *Z* or *E* product then occurs following crossing onto the ground-state potential energy surface. Both of these nuclear rearrangements are necessarily energetically downhill processes, requiring dissipation of energy as heat, and cannot be avoided without a concomitant energy cost elsewhere. As the excited state of dba-Z-1 is quenched by energy transfer to open the gate, therefore, the information regarding the macrocycle's (probable) location is erased on decay of the initial, vertically excited state to the perpendicular intermedi-

ate. Thus the part of the mechanism of **1** that intrinsically requires dissipation of energy is equivalent to the erasure of the information known to a gate-operating demon, in agreement with Bennett's resolution²⁷ of the Maxwell demon paradox.

Various methods for the net transport of macrocycles between the binding sites in rotaxanes have previously been demonstrated in the form of stimuli-responsive molecular shuttles^{2,5,8,11,12}. However, these are simple two-state switches^{28,29}, the most basic and functionally limited type of machine mechanism in which the ring distribution is always at, or relaxing towards, equilibrium. In contrast, biological motors and machines use mechanisms that operate far from equilibrium¹. During the past decade, statistical physics has developed a number of theoretical mechanisms that explain how the transport of brownian particles away from equilibrium can occur. These so-called 'brownian ratchet' mechanisms fall into two general classes: energy ratchets³⁰, in which the energy minima and maxima of the potential energy surface are varied irrespective of the particle's location; and information ratchets^{20–22}, where the energy maxima (kinetic barriers to motion) change according to the position of the particle. The energy ratchet concept has recently been used to design some of the first synthetic molecular machines that are more complex than simple switches^{9,28}, but rotaxane **1** is the first example of a synthetic molecular information ratchet. For an information ratchet to function it is unnecessary for the binding affinities of the two compartments to be as similar as they are in **1** (although it affects the efficiency of the mechanism²²); the point is that the particle distribution can be driven away from whatever the equilibrium value is. From the perspective of synthetic molecular machine design, the situation in which the two sites have significantly different binding affinities may prove particularly important because this corresponds to a route by which particles can be pumped energetically uphill against an opposing force.

Received 9 June; accepted 15 November 2006.

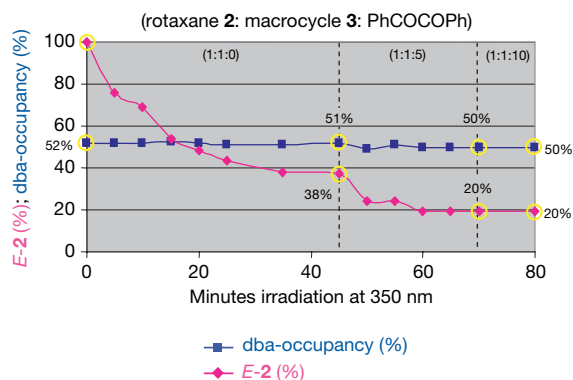
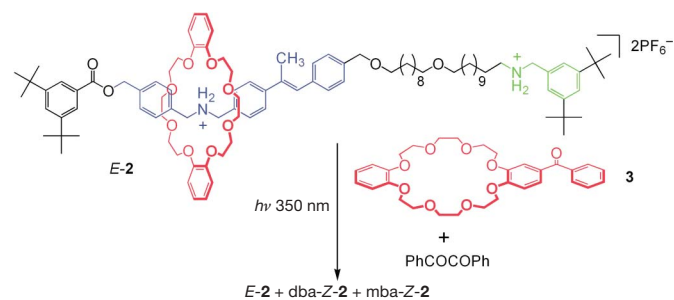


Figure 4 | Operation of rotaxane 2, featuring only intermolecular photosensitization of the α -methyl stilbene gate. The plot shows the change in the *E:Z* ratio (*E-2* (%), shown by purple diamonds) and the dba:mba ratio (dba-occupancy (%), shown by dark blue squares) that occurs during irradiation of **2**+**3** (1:1) at 350 nm in CD₃OD, 298 K in the absence and presence (5 and 10 equiv.) of benzil. There is a small amount (<2%) of photodegradation over the course of the experiment, and the error in the final *E:Z* and dba:mba ratios is $\pm 2\%$.

- Schliwa, M. (ed.) *Molecular Motors* (Wiley-VCH, Weinheim, 2003).
- Bissell, R. A., Córdova, E., Kaifer, A. E. & Stoddart, J. F. A chemically and electrochemically switchable molecular shuttle. *Nature* **369**, 133–137 (1994).
- Kelly, T. R., De Silva, H. & Silva, R. A. Unidirectional rotary motion in a molecular system. *Nature* **401**, 150–152 (1999).
- Koumura, N., Zijlstra, R. W. J., van Delden, R. A., Harada, N. & Feringa, B. L. Light-driven monodirectional molecular rotor. *Nature* **401**, 152–155 (1999).
- Brouwer, A. M. et al. Photoinduction of fast, reversible translational motion in a hydrogen-bonded molecular shuttle. *Science* **291**, 2124–2128 (2001).
- Leigh, D. A., Wong, J. K. Y., Dehez, F. & Zerbetto, F. Unidirectional rotation in a mechanically interlocked molecular rotor. *Nature* **424**, 174–179 (2003).
- Thordarson, P., Bijsterveld, E. J. A., Rowan, A. E. & Nolte, R. J. M. Epoxidation of polybutadiene by a topologically linked catalyst. *Nature* **424**, 915–918 (2003).
- Badjić, J. D., Balzani, V., Credi, A., Silvi, S. & Stoddart, J. F. A molecular elevator. *Science* **303**, 1845–1849 (2004).
- Hernández, J. V., Kay, E. R. & Leigh, D. A. A reversible synthetic rotary molecular motor. *Science* **306**, 1532–1537 (2004).
- Fletcher, S. P., Dumur, F., Pollard, M. M. & Feringa, B. L. A reversible, unidirectional molecular rotary motor driven by chemical energy. *Science* **310**, 80–82 (2005).
- Liu, Y. et al. Linear artificial molecular muscles. *J. Am. Chem. Soc.* **127**, 9745–9759 (2005).
- Berná, J. et al. Macroscopic transport by synthetic molecular machines. *Nature Mater.* **4**, 704–710 (2005).
- Shirai, Y., Osgood, A. J., Zhao, Y., Kelly, K. F. & Tour, J. M. Directional control in thermally driven single-molecule nanocars. *Nano Lett.* **5**, 2330–2334 (2005).
- Elkema, R. et al. Molecular machines: Nanomotor rotates microscale objects. *Nature* **440**, 163 (2006).
- Muraoka, T., Kinbara, K. & Aida, T. Mechanical twisting of a guest by a photoresponsive host. *Nature* **440**, 512–515 (2006).
- Maxwell, J. C. Letter to P. G. Tait, 11 December 1867. Reproduced in *The Scientific Letters and Papers of James Clerk Maxwell* Vol. II, 1862–1873 (ed. Harman, P. M.) 331–332 (Cambridge Univ. Press, Cambridge, UK, 1995).
- Maxwell, J. C. *Theory of Heat* Ch. 22 (Longmans, Green and Co., London, 1871).
- Maxwell, J. C. Letter to P. G. Tait, circa. 1875. Reproduced in *The Scientific Letters and Papers of James Clerk Maxwell* Vol. III, 1874–1879 (ed. Harman, P. M.) 185–187 (Cambridge Univ. Press, Cambridge, UK, 2002).
- Leff, H. S. & Rex, A. F. (eds) *Maxwell's Demon 2. Entropy, Classical and Quantum Information, Computing* (Institute of Physics Publishing, Bristol, 2003).
- Astumian, R. D. & Derényi, I. Fluctuation driven transport and models of molecular motors and pumps. *Eur. Biophys. J.* **27**, 474–489 (1998).

21. Parmeggiani, A., Jülicher, F., Ajdari, A. & Prost, J. Energy transduction of isothermal ratchets: Generic aspects and specific examples close to and far from equilibrium. *Phys. Rev. E* **60**, 2127–2140 (1999).
22. Parrondo, J. M. R. & De Cisneros, B. J. Energetics of Brownian motors: A review. *Appl. Phys. A* **75**, 179–191 (2002).
23. Tokunaga, Y., Akasaka, K., Hisada, K., Shimomura, Y. & Kakuchi, S. A rotaxane synthesis based on stilbene photoisomerization. A photoswitchable catch and release process. *Chem. Commun.* 2250–2251 (2003).
24. Kolchinski, A. G., Busch, D. H. & Alcock, N. W. Gaining control over molecular threading: benefits of second coordination sites and aqueous–organic interfaces in rotaxane synthesis. *J. Chem. Soc. Chem. Commun.* 1289–1291 (1995).
25. Ashton, P. R. *et al.* Dialkylammonium ion/crown ether complexes: the forerunners of a new family of interlocked molecules. *Angew. Chem. Int. Edn Engl.* **34**, 1865–1869 (1995).
26. Hammond, G. S. *et al.* Mechanisms of photochemical reactions in solution. XXII. Photochemical *cis–trans* isomerization. *J. Am. Chem. Soc.* **86**, 3197–3217 (1964).
27. Bennett, C. H. The thermodynamics of computation – a review. *Int. J. Theor. Phys.* **21**, 905–940 (1982).
28. Chatterjee, M. N., Kay, E. R. & Leigh, D. A. Beyond switches: ratcheting a particle energetically uphill with a compartmentalized molecular machine. *J. Am. Chem. Soc.* **128**, 4058–4073 (2006).
29. Kay, E. R. & Leigh, D. A. Lighting up nanomachines. *Nature* **440**, 286–287 (2006).
30. Reimann, P. Brownian motors: Noisy transport far from equilibrium. *Phys. Rep.* **361**, 57–265 (2002).

Supplementary Information is linked to the online version of the paper at www.nature.com/nature.

Acknowledgements We thank P. J. Camp and his research group for the free energy calculation, and the EPSRC, the EU project Hy3M and the Carnegie Trust for financial support. D.A.L. is an EPSRC Senior Research Fellow and holds a Royal Society-Wolfson research merit award.

Author Contributions V.S., C.-F.L. and E.R.K. contributed equally to this work.

Author Information Reprints and permissions information is available at www.nature.com/reprints. The authors declare no competing financial interests. Correspondence and requests for materials should be addressed to D.A.L. (David.Leigh@ed.ac.uk).